Available online at www.sciencedirect.com

SciVerse ScienceDirect

Ceramics International 38 (2012) 2733–2741

CERAMICS
INTERNATIONAL

www.elsevier.com/locate/ceramint

Dispersion and co-dispersion of ZrB_2 and SiC nanopowders in ethanol

Xinghong Zhang [a], Yang Hou [a,*], Ping Hu [a,*], Wenbo Han [a], Junting Luo [b]

[a] National Key Laboratory of Science and Technology on Advanced Composites in Special Environment, Harbin Institute of Technology, Harbin 150001, PR China
[b] State Key Laboratory of Metastable Materials Science and Technology, Yanshan University, Qinhuangdao 066004, PR China

Received 13 September 2011; received in revised form 14 November 2011; accepted 15 November 2011
Available online 25 November 2011

Abstract

The dispersion and co-dispersion behavior of ZrB_2 and SiC nanopowders in ethanol solution was studied by sedimentation test, particle size measurement and transmission electron microscope (TEM) analysis. The dispersion behavior of ZrB_2 and SiC nanopowders in ethanol solution was strongly dependent on the pH values, types and amounts of dispersant. PEI was found to be effective for the dispersion of both ZrB_2 and SiC nanopowders in ethanol solution. With the addition of PEI, the isoelectric points of ZrB_2 and SiC nanopowders in ethanol solution were at pH 10 and pH 9.5, and shift to pH 13 and pH 12.3, respectively. The stability of ZrB_2 suspension increased with the dispersant content increasing until reached 0.7 wt% and well-dispersed SiC slurry can be obtained with more than 2.5 wt% PEI. The suitable pH value for the dispersion of ZrB_2 and SiC nanopowders should be lower than 12 and 10, respectively. The well co-dispersed ZrB_2 and SiC nanocomposite powders can be achieved by using 1 wt% or more PEI below pH 10.

Keywords: B. Composites; C. Chemical properties; D. Borides; Dispersion

1. Introduction

The interest in ultra-high temperature ceramics (UHTCs) has increased significantly in recent years [1,2] due to their remarkable properties, such as high melting point, high thermal conductivities, excellent corrosion resistance and good oxidation resistance [3,4], which make them promising candidates for high-temperature structural applications. Among the UHTCs, a lot of works have been performed on ZrB_2–SiC ceramics which are produced by micron-sized ZrB_2 and SiC powders [5,6]. Nanocrystalline materials are expected to show a much higher performance than their counterpart conventional coarse-grained polycrystalline materials in the light of the well-known strengthening mechanism, called grain boundary strengthening or fine-grain strengthening [7]. In order to acquire UHTCs with good properties, nano-sized ZrB_2 and SiC powders should be studied and applied. It has been reported that ZrB_2 + 20 vol.% SiC nanocomposite has excellent mechanical properties (high flexural strength and fracture toughness) which were strongly dependent on the formation of the unusual intragranular nanostructures [8,9].

With the development of materials, nanoparticles as raw materials play an important role in improving the function of traditional material. However, nanoparticles easily arise agglomerate or absorbed other particles to make it lose particular surface performance owing to the large surface area, high surface energy, and high activity during preparation, storage and using process, which lead to bad performance in the process of actual using [10,11]. The solving method of agglomeration and dispersibility problem of nanopowders is a key technology for preparing and developing high quality materials [12,13].

As for the fabrication of ZrB_2 and SiC nano-composites, the preparation of well-dispersed ceramic slurries is one of the most important step in order to guarantee a uniform mixing. Dispersion behaviors of ZrB_2 and SiC micron and submicron powders in aqueous solution have been analyzed in the previous work [14,15]. Although aqueous processing is environmental friendly and inexpensive, when taking into account the reaggregation of nanopowder during drying process, ethanol has the advantage as compared to water which is attributed to its low surface tension. Moreover, as for fabrication of products, wet processes such as ball milling, mixing and slurry preparation are

---

* Corresponding authors. Tel.: +86 451 86402382; fax: +86 451 86402382.
E-mail addresses: conan19821025@163.com (Y. Hou), huping@hit.edu.cn (P. Hu).

0272-8842/$36.00. Crown Copyright © 2011 Published by Elsevier Ltd and Techna Group S.r.l. All rights reserved.
doi:10.1016/j.ceramint.2011.11.042

often required. Oxides on the powder surface formed by corrosion during processing may introduce impurities and promote grain growth [16,17], thus lead to performance degradation. The corrosion behavior of powder during wet processing can be trailed off in ethanol compared with aqueous solution [18,19]. However, up to now, the information about the co-dispersion of ZrB_2 and SiC nanopowders in ethanol solution is still unavailable.

In the present research, the dispersion behavior of ZrB_2 and SiC nanopowders in ethanol solutions was investigated with the use of three kinds of dispersants (Solspers20000, NK-1 and PEI(10000)) which can be well-dissolved in ethanol. Although, many effective dispersants have been applied in aqueous, such as polymer acrylic acid (PAA), and polymethacrylic acid (PMAA) [14,20] few of them can fully dissolved in ethanol at room temperature. The purpose of this paper was to discuss the influence of different pH values as well as different dispersant types and dosages on the dispersion behavior of ZrB_2 and SiC nanopowders in ethanol solution and obtain the suitable pH range and content of dispersant, then prepare well-dispersed composite slurry and analyze the co-dispersion of ZrB_2 and SiC nanocomposite powders.

2. Experimental procedures

2.1. Materials

Commercially available ZrB_2 nanopowder (the primary particle size was 60 nm, purity >95%, oxygen content 0.75 wt%, Kaier Nanometer Energy & Technology Co. Ltd., Hefei, China) and SiC nanopowder (the primary particle size was 40–50 nm, Kaier Nanometer Energy & Technology Co. Ltd., Hefei, China) were used as raw materials. Three dispersants were used, one was Solspers20000, produced by the Lubrizo Company. The second was polyethylene imine (PEI, Aladdin Co. Ltd., Shanghai, China), a cationic polymer with an average molecular weight of 10,000. The third is NK-1(micro/nanopowder dispersant). Absolute ethyl alcohol with a water level around 0.1% as a solvent for all the suspensions.

2.2. Suspension preparation

The suspensions used for all measurements were prepared by adding the as-received powder to ethanol at selected powder mass percentages. The dosage of added dispersant was expressed as a dry weight percentage of powder basis (dwb%). The procedure for preparing the suspensions can be described as follows:

Step 1: The dry powder was slowly added to the premixed solution with the desired dispersant content.
Step 2: The suspension was then ultrasonically deflocculated (JYD-801, Jiatuanda Technology Co. Ltd., Shenzhen, China) at an output power of 160 W in an ice bath.
Step 3: The suspension was ball milled after ultrasonication, with SiC balls (diameter: 2–3 mm) as the ball milling media at 400 rpm for 10 h.

2.3. Zeta potential and particle size measurements

Zeta potential measurements (Malvern Zetasizer Molecular Size, Molecular Wight & Zeta Potential Analyzers, UK) were performed for the 0.01 vol.% ZrB_2 and SiC suspensions with or without the desired quantity of PEI. The zeta potential was recorded as a function of the pH of the suspension. The acidity of solution was regulated by glacial acetic acid (HAc) and tetramethyl ammonium hydroxide (TMAH) (10% in methanol). The pH value was measured with a pH meter (PHSJ-3F, CANY Co. Ltd., Shanghai, China) at room temperature. Since the lack of standard buffer solutions for ethanol, the pH meter determined the so-called ''operational pH values'' for non-aqueous solvents which was used in this paper [21].

The average particle size of the powders was determined using a laser particle size analyzer (Hylology Instruments Co. Ltd., Dandong, China). Suspensions containing 2 wt% of powders were prepared with different kinds, amounts and pH values of dispersants in ethanol solution.

2.4. Adsorption measurement and sedimentation test

The adsorption isotherms of the dispersant used with the ZrB_2 and SiC nanopowders were obtained by elemental analysis (Vario EL/micro cube, Elementar Co. Ltd., Germany). Dispersant at various amounts were added to a certain amount of powders in solvent. After the mixing, the dispersion medium and any excess dispersant were removed from the ZrB_2 and SiC nanopowders by centrifugation at 3500 rpm for 3 h. The remaining ZrB_2 and SiC nanopowders and adsorbed dispersant were dried in a convection oven at 60 °C for 24 h, and the mass percent of nitrogen element of the dried ZrB_2 and SiC nanopowders was analyzed to determine the amount of dispersant retained.

Sedimentation measurements were carried out by drawing samples of the 2 wt% ZrB_2 and SiC suspensions into cuvette and then covering with a cap to avoid the evaporation. After sedimentation for 1 day, the stabilities of the suspensions were recorded by analysing the height of turbid fluid.

3. Results and discussion

The suspension which contains the Solspers20000 was completely clear after sedimentation for 1 day (Fig. 1a and b). This phenomenon indicated that Solspers20000 was not suitable for dispersing ZrB_2 and SiC nanopowders. The dispersion behavior with NK-1 and PEI was further characterized by particle size measurements. The frequency curve of PEI in Fig. 2 was in the range below 1 μm and the average particle size of ZrB_2 and SiC nanopowders was much smaller than that of NK-1. Therefore, PEI was chosen as the dispersant for the dispersion and co-dispersion of ZrB_2 and SiC nanopowders in ethanol solution. The optimum content of PEI for the dispersion of ZrB_2 and SiC nanopowders in ethanol solution was subsequently analyzed. The sediment volume of ZrB_2 suspension was high when the addition of PEI ranging from 0.1 wt% to 0.5 wt% (Fig. 3). The average particle size

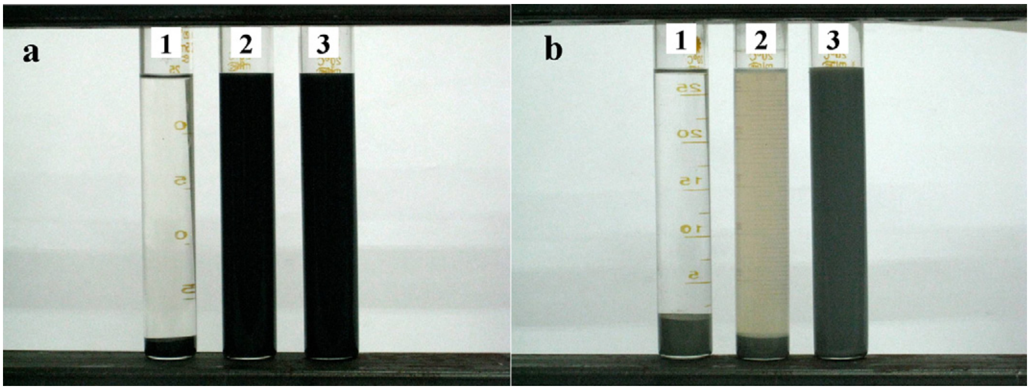

Fig. 1. Photograph of the 2 wt% ZrB_2 and SiC suspensions after sedimentation for 1 day with different dispersants (pH = 8): (a) ZrB_2; (b) SiC. (1) Solspers20000; (2) NK-1; (3) PEI10000.

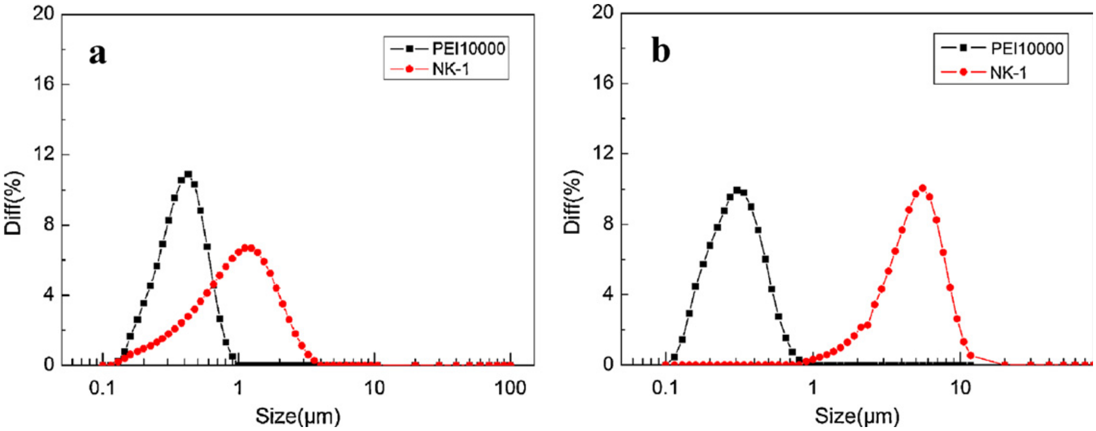

Fig. 2. Size distribution of powder after the addition of dispersants: (a) ZrB_2; (b) SiC.

decreased with increasing the dosage of PEI until reached 0.7 wt% and kept stable during further accession of dispersant (Fig. 4) which was in agreement with Fig. 3. When 0.7 wt% or more PEI was added into ZrB_2 suspension, there was no obvious sedimentation and the D_{50} was stabilized at about 0.33 μm.

The sediment volume of SiC suspension decreased as the content of dispersant increased (Fig. 5) and the particle size distribution ranged from 0.1 to 10 μm when the addition of PEI up to 2 wt% (Fig. 6a). Although the average particle size decreased significantly when comparing with those containing 1 wt% or without dispersant (Fig. 6b), the sediment volume was

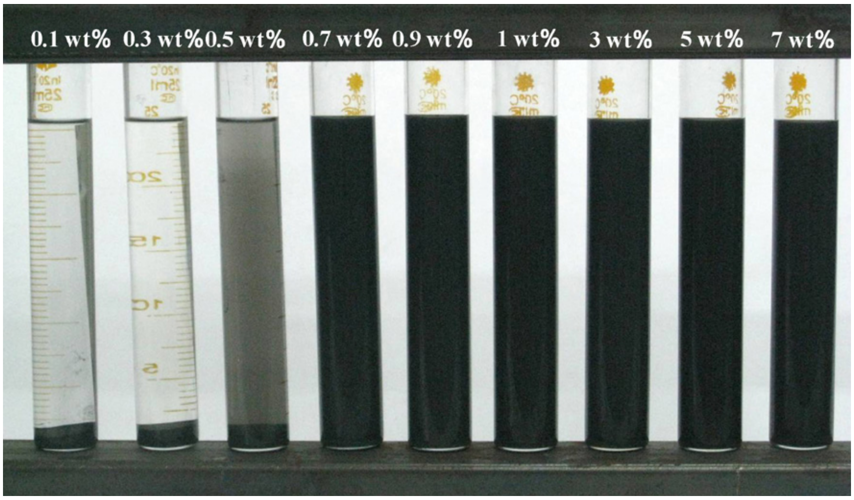

Fig. 3. Photograph of the 2 wt% ZrB_2 suspension after sedimentation for 1 day with different PEI contents. The numbers at the top of the cuvette denotes the content of PEI in dwb% (pH = 8).

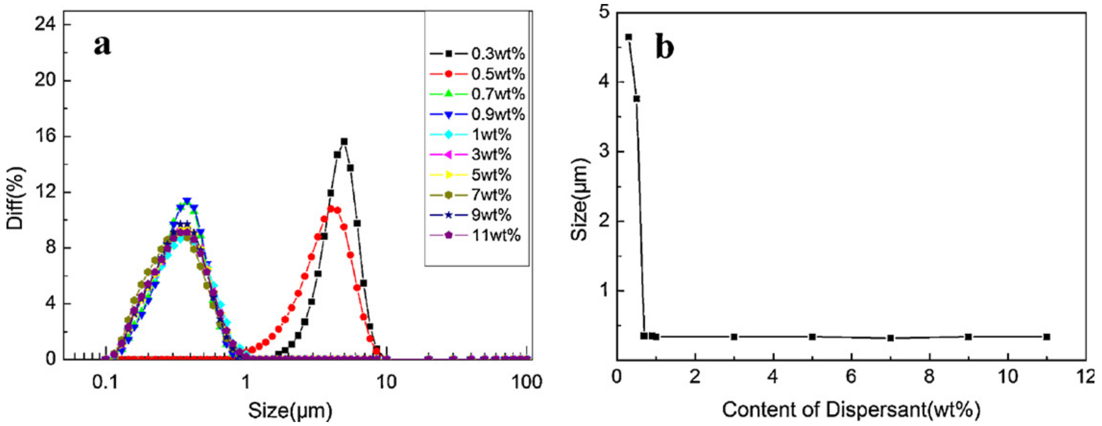

Fig. 4. Size distribution and variation of ZrB_2 powder with different PEI contents (pH = 8): (a) size distribution; (b) size variation.

still high after sedimentation for 1 day which indicates the dispersion was nonhomogeneous. A constant value of SiC suspension can be achieved until the dosage of the PEI reaching 2.5 wt% which followed the same trend as ZrB_2 suspension.

The oblique line in Fig. 7 represents the complete adsorption of PEI on the particle surfaces. Almost all the PEI was adsorbed onto the solid surface when the dosage of PEI was less than 0.7 wt%, suggesting the high adsorption affinity of the PEI with the ZrB_2 particles. However, when adding more than 0.7 wt% PEI, the adsorption curve reached a plateau corresponding to the saturated adsorption. Once the accession of PEI exceeded the saturation limit, the adsorption amount did not increase remarkably and some PEI molecules were remained in the solvent as free polymer.

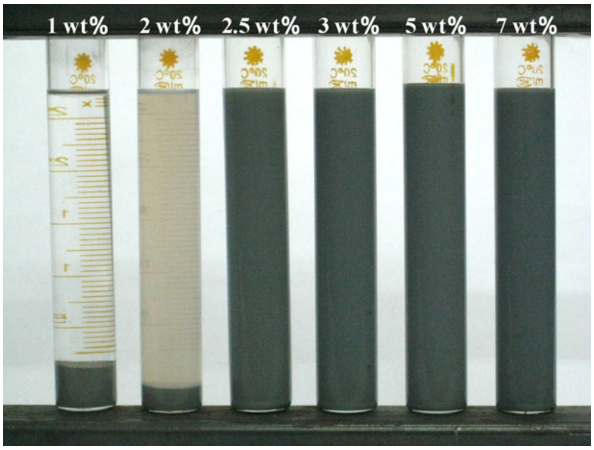

Fig. 5. Photograph of the 2 wt% SiC suspension after sedimentation for 1 day with different PEI contents. The numbers at the top of the cuvette denotes the content of PEI in dwb% (pH = 8).

When the accession of PEI was less than 0.7 wt% during dispersed ZrB_2, the particle surface cannot be fully covered with the dispersant. The vacancy that was not been covered would absorb each other and induce flocculation of particles. So the quantity of PEI that adding into the suspensions should be greater than or equal to the amount of saturated adsorption. The similar behavior can be deduced for the dispersion of SiC nanopowder.

PEI has a branched structure and there are some branched long chains of PEI not adsorbed on a surface. The non-adsorbed long chains promote the steric repulsive force between solid surfaces. The increase in steric repulsive force attribute to the formation of the loop structure and the non-adsorbed long branched chain will facilitate the dispersion of aggregates in a suspension [22].

The zeta potential curves as a function of pH for the 0.01 vol.% ZrB_2 with or without dispersant in ethanol

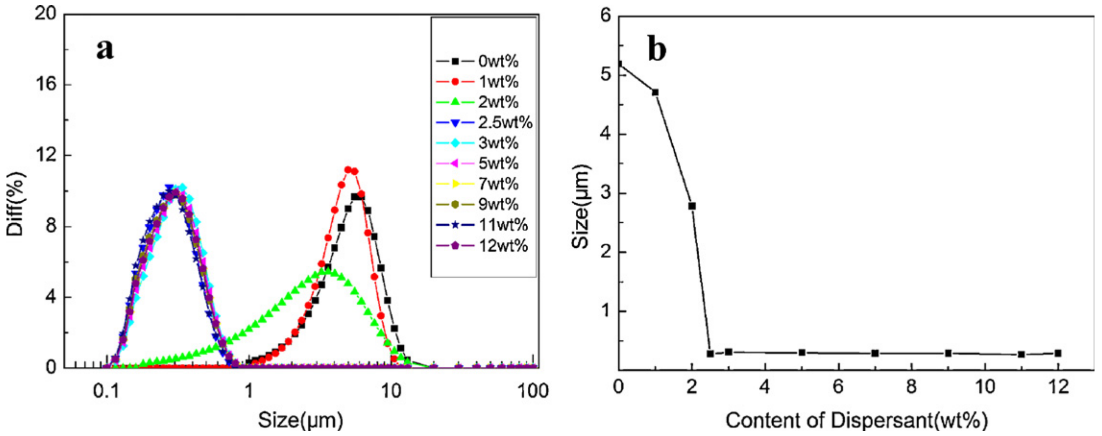

Fig. 6. Size distribution and variation of SiC powder with different PEI contents (pH = 8): (a) size distribution; (b) size variation.

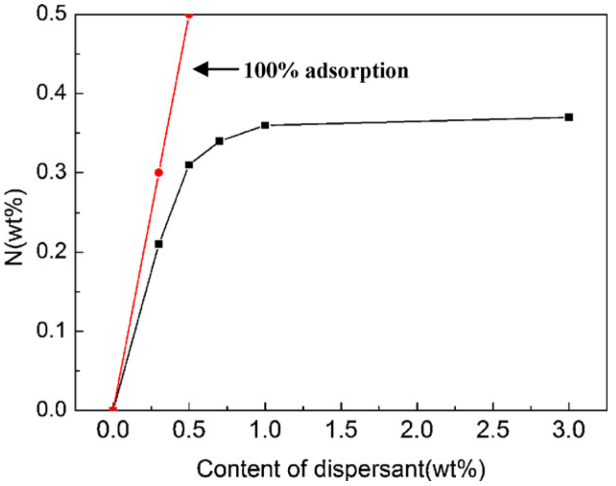

Fig. 7. Amount of adsorbed PEI on ZrB_2 nanopowder as a function of added PEI (pH = 8).

suspension is displayed in Fig. 8a. In the absence of dispersant, the isoelectric point (IEP) for ZrB_2 nanopowders in ethanol solution was found to be at pH 10 and the zeta potential was about 10 mV in the pH range of 4–9. With the accession of PEI, the adsorption of PEI onto the surface shifted the IEP from pH 10 to approximately pH 13 and the zeta potential was raised to 12 mV. The zeta potential of SiC powder was positive under the condition of $pH < 9.5$ in the absence of dispersant (Fig. 8b). When adding PEI into the solution, the IEP of SiC moved from pH 9.5 to approximately pH 12.3 and the highest value of the zeta potential of SiC increased from 7.5 to 13 mV in the acidic and neutral pH region.

It was proved that there were large differences in dissociation behavior depending on media by comparing the isoelectric points and zeta potential of ZrB_2 and SiC nanopowders in ethanol with the corresponding values in aqueous solutions [23,24]. In ethanol solution the IEP of ZrB_2 and SiC nanopowders transferred to higher values and the values of zeta potential were lower than that in aqueous solution.

The stability of ZrB_2 with 1 wt% PEI and SiC with 2.5 wt% PEI suspensions under different pH values were determined by the sedimentation test (Fig. 9). Well-stabilized ZrB_2 and SiC suspensions can be observed ranging from pH 4 to 9. However, the SiC suspension became unstable with further increasing pH value compared with ZrB_2 suspension. When the pH was raised to 12, both ZrB_2 and SiC suspensions exhibited completely sediment characteristic, resulting from the low surface charge of ZrB_2 and SiC particles.

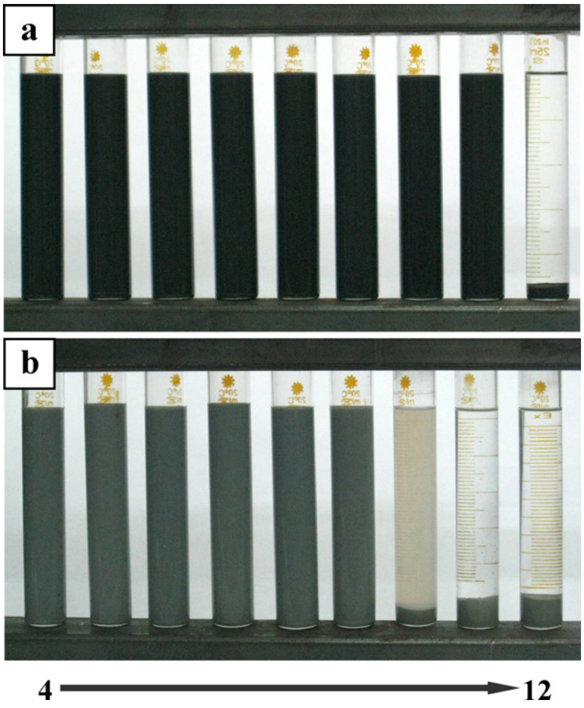

Fig. 9. Photograph of the 2 wt% ZrB_2 and SiC suspensions after sedimentation for 1 day with different pH values. The pH was increased from 4 to 12, interval of 1 during the tests: (a) ZrB_2 with 1 wt% PEI; (b) SiC with 2.5 wt% PEI.

The particle size distribution of ZrB_2 suspension with 1 wt% PEI remained stable in the pH region of 4–11 and the D_{50} of ZrB_2 powder was about 0.33 μm (Fig. 10). The particle size distribution of SiC suspension with 2.5 wt% PEI had the same tendency as the ZrB_2 suspension in the pH range of 4–9, but the average particle size increased from pH 10 to 12, which implied that the particles were agglomerating with each other in this case (Fig. 11). The particle size measurement was consistent

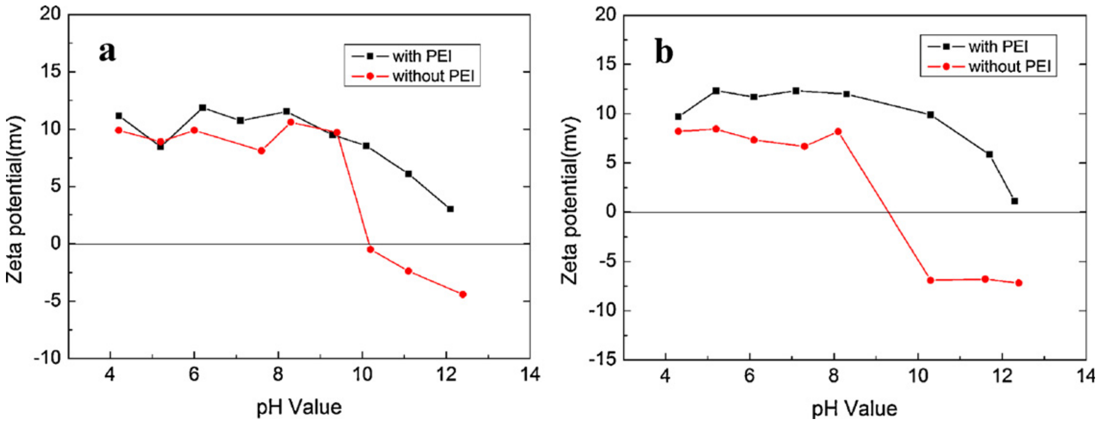

Fig. 8. Zeta potential of powders in the presence and absence of dispersant in ethanol solution: (a) ZrB_2; (b) SiC.

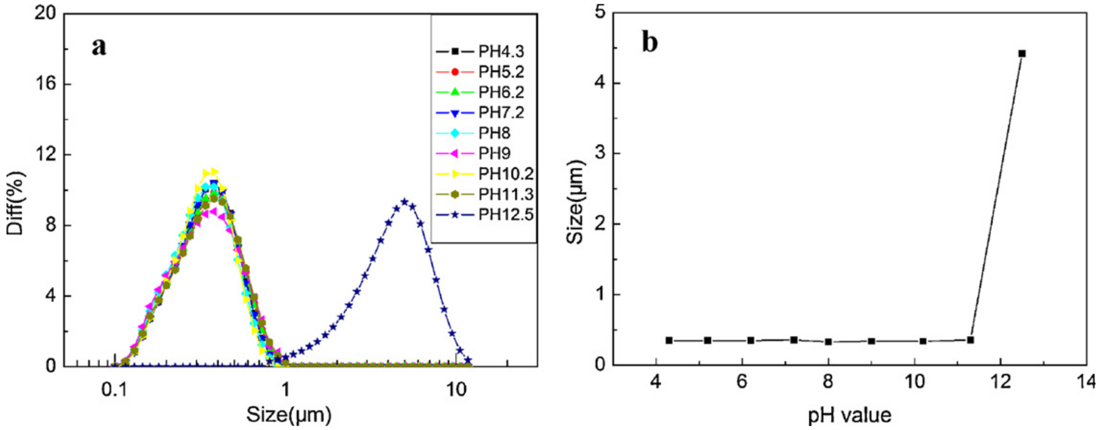

Fig. 10. Size distribution and variation of ZrB_2 powder with different pH values (1 wt% PEI): (a) size distribution; (b) size variation.

with the sedimentation test which was shown in Fig. 9. This indicated that ZrB_2 and SiC nanopowders can be co-dispersed with PEI as the dispersant below pH 10.

The dispersion behavior of ZrB_2 and its oxide in aqueous solution has been studied by many researchers. Lee et al. has reported that the viscosity of the concentrated ZrB_2 slurry decreased with the addition of PEI(10000) up to 1.5 wt%, and keep steady in the pH range of 3–9 in aqueous solution [23]. The average particle size of zirconia powder dispersed with PEI as a function of pH has been studied by Tang et al. [25]. The particle is in a monodispersed state in the range of $\mathrm{pH} < 10$ and agglomerated at $\mathrm{pH} > 10$. This was demonstrated that ZrB_2 can be dispersed in aqueous solution in the pH range below 10 which is similar as dispersing in ethanol solution.

Under strong acidic conditions ($\mathrm{pH} < 2$) and strong basic conditions ($\mathrm{pH} > 11$), more acid and alkali are needed to adjust the pH values and zeta potential has a tendency to decrease, which can be explained by DLVO theory [26]. The increased ionic strength in the suspension compresses the thickness of double electric layer and results in the decrease of zeta potential of the powder.

The IEP of ZrB_2 and SiC nanopowders in ethanol suspension was strongly affected by the addition of PEI. The surface was positively charged in the pH range below 13. This can be attributed to PEI which was a cationic polyelectrolyte and has a molecular structure as follows [27]:

$$(-CH_2-CH_2-NH-)_n$$

In acidic and weakly basic regions, PEI was a positively charged polyelectrolyte; hence the chemisorption of PEI on particle surface might lead to charge reversal which owing to the protonation of the amine group in the molecule [28,29].

The process that conferred positive charge on the polymer skeleton was according to the reaction:

$$(-CH_2-CH_2-NH-)_n + H_3O^+ \\ \rightarrow (-CH_2-CH_2-NH_2{}^+-)_n + H_2O$$

The positively charged $-NH^{2+}$ groups of PEI produced by adsorbing H^+ ions in ethanol solution can be easily adsorbed on the negatively charged particle surface which results in the IEP move to more alkaline pH value [25]. Furthermore, owing to the electrostatic repulsion between the highly ionized $-NH^{2+}$ groups, the adsorbed polymers tended to extend their long chain polymer backbone into solutions, leading to an increase in the steric repulsive force [30].

Particles may be stable in suspension either because of their charge and consequent repulsion (electrostatic stabilization) or

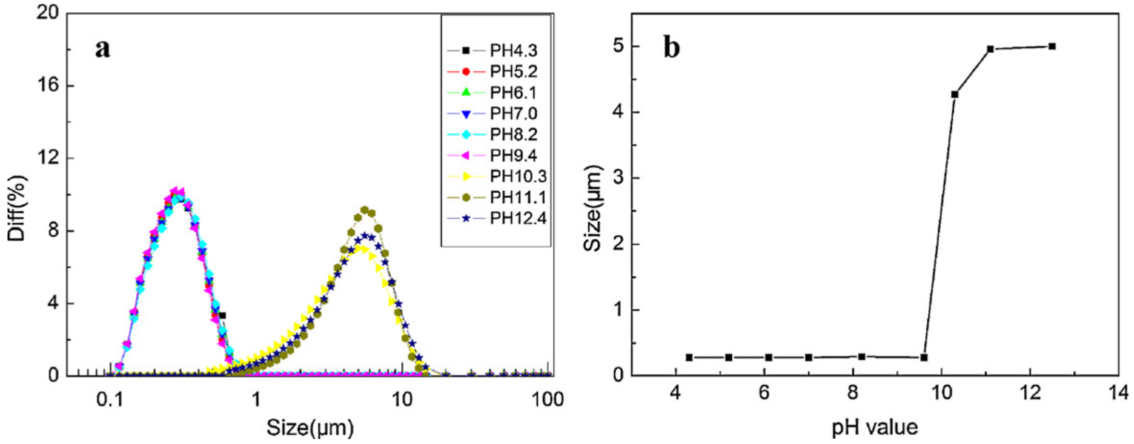

Fig. 11. Size distribution and variation of SiC powder with different pH values (2.5 wt% PEI): (a) size distribution; (b) size variation.

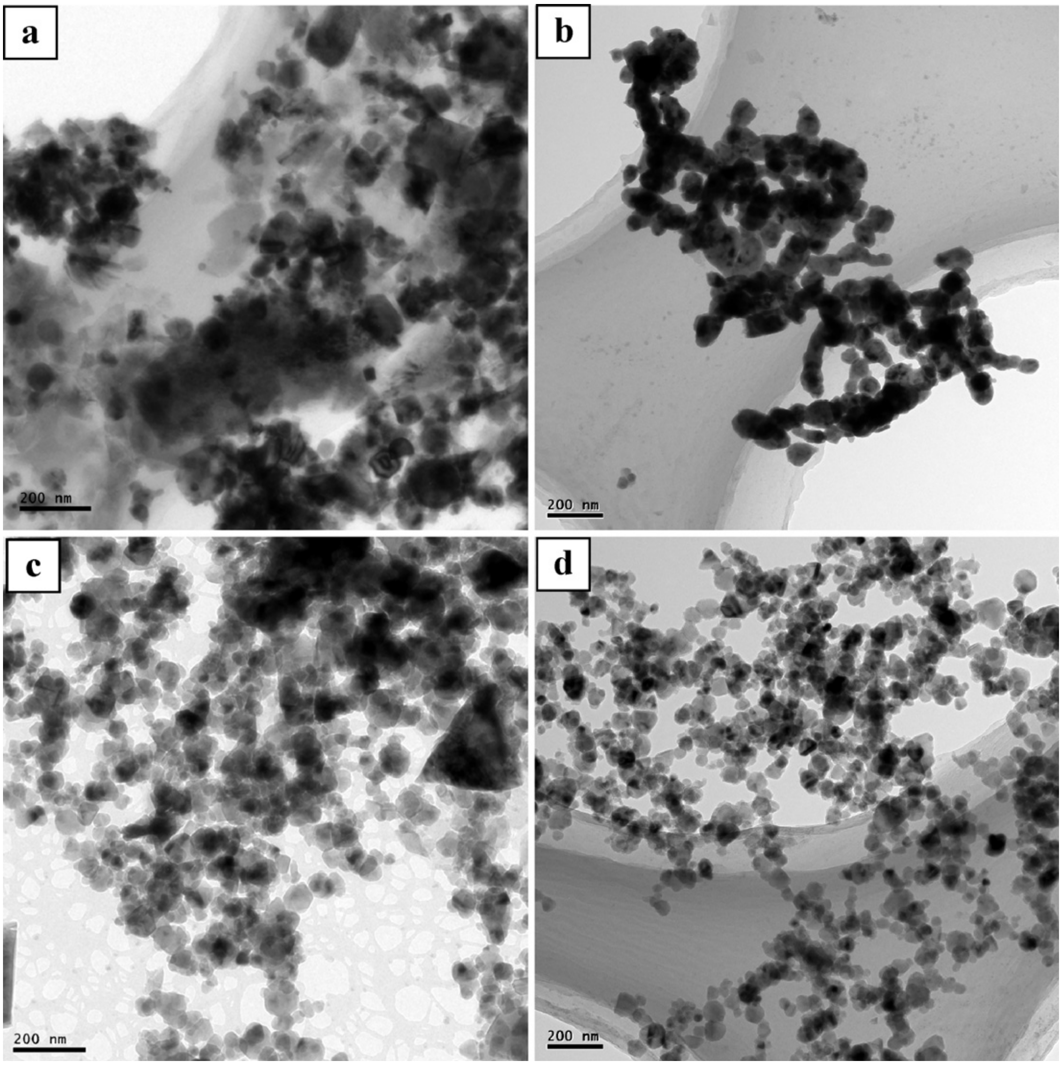

Fig. 12. TEM images of ZrB_2 and SiC in the presence and absence of dispersant in ethanol solution (pH = 8): (a) ZrB_2 without PEI; (b) ZrB_2 with 1 wt% PEI; (c) SiC without PEI; (d) SiC with 2.5 wt% PEI.

as a result of the presence of adsorbed polymer layers (steric stabilization). Electrostatic stabilization is thought to be the most effective in high-dielectric-constant media [31]. Correspondingly, many researchers have reported that the steric repulsion among particles promotes a dominant dispersibility and stability in nonaqueous suspension as the low dielectric constant [22].

The results of our dispersion experiments indicated that the ZrB_2 and SiC nanopowders can be well-dispersed below pH 10 and badly agglomerated near IEP. This phenomenon was corresponding to the zeta potential curve. In general, the higher the absolute value of the zeta potential, the higher the charge density is on the surface of powders and the larger the repulsion among particles [32]. When dispersing ZrB_2 and SiC nanopowders in ethanol media, although the electrostatic repulsion energy was less than that in aqueous solution because of the low ionic concentration and the low dielectric constant [25], the importance of pH value and electrostatics in ethanol media cannot be neglected.

Based on the above results, the absorption of the dissociated dispersant might increase the surface charge density and the electrostatic repulsion force among particles, which was validated by the zeta potential measurement. Furthermore, the longer chain polymer backbone anchored on the surface of ZrB_2 and SiC particles or stretched out into the solutions also caused the stabilization of the slurries by steric repulsion. The combination of electrostatic and steric stabilization in the presence of dispersant will be more effective for obtaining well-dispersed slurries [30].

The TEM analysis displays that the dispersibility of ZrB_2 and SiC nanopowders was poor without the accession of PEI (Fig. 12a and c). The dispersant adsorbed on nanoparticle surfaces enhanced dispersibility and decreased agglomerates significantly (Fig. 12b and d). Adjacent nanoparticles tend to aggregate to form agglomerations in solution due to strongly omnipresent van der Waals attractions. When adsorbed on ZrB_2 and SiC nanoparticles surface, PEI will prominently improved the repulsive forces between particles by electrostatic and steric effects. The attractions which caused agglomerates were enormously exceeded by the polymer enhanced repulsions [33], and the dispersibility of nanoparticles increased accordingly.

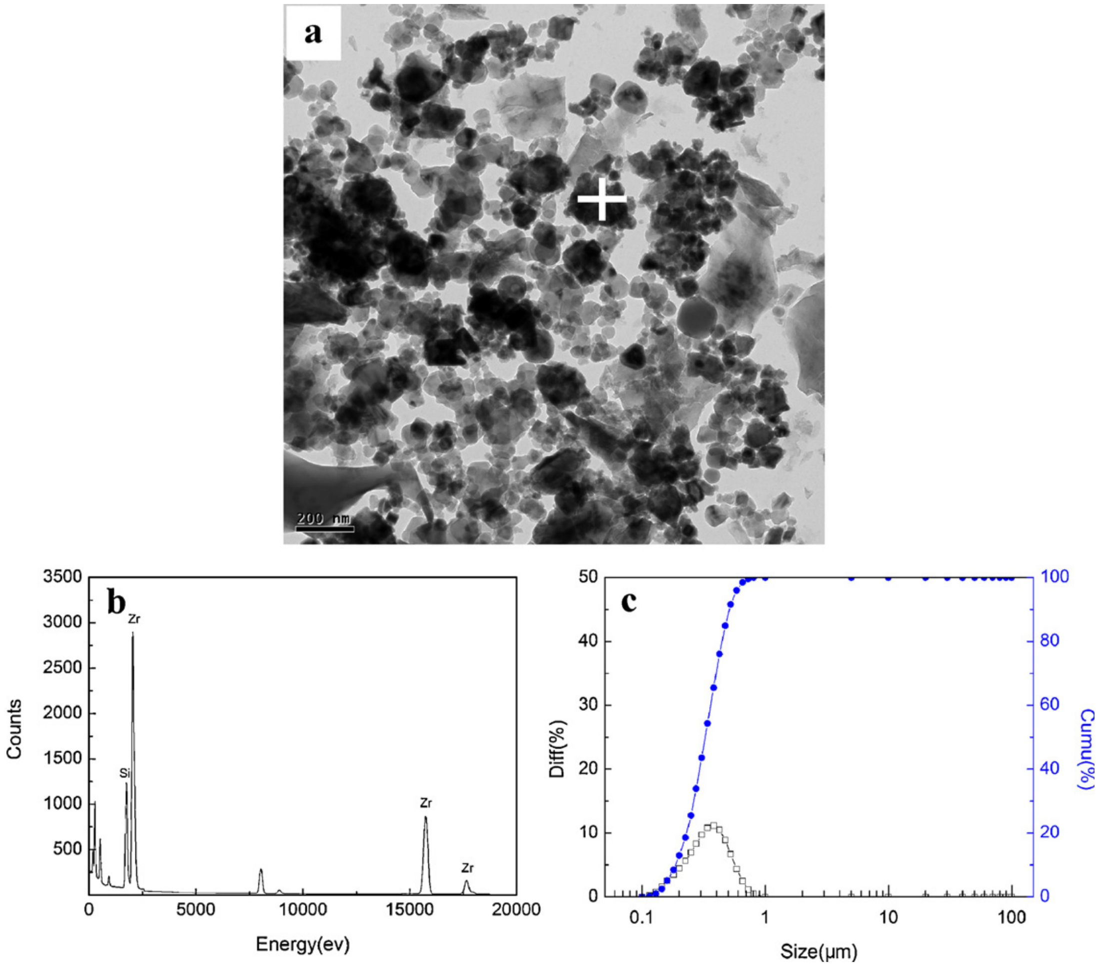

Fig. 13. The dispersion property of ZrB_2 + 20 vol.% SiC after treatment in ethanol solution: (a) TEM image; (b) EDS analysis (as indicated by cross in (a)); (c) size distribution.

The dispersion of compound slurry that mixed by a variety of powders is much more difficult to achieve than single-phase component, because the surface characteristics of powders are different from each other. Furthermore, the particle sizes and the pH ranges of stabilization are also different, so that it would result in complex interactions among different particles in the solvent.

ZrB_2 and SiC nanopowders had the similar surface behavior and can be well-dispersed, respectively by electrostatic and steric repulsion with adding the suitable dosage of PEI below pH 10. On the basis of single-phase dispersion experiment, ZrB_2 + 20 vol.% SiC suspensions was prepared at pH 8 with 1 wt% PEI and ball milling for 10 h. Fig. 13a shows that the two kinds of particles were dispersed with themselves and each other. The ZrB_2 and SiC particles cannot be clearly distinguished as their similar shapes and contrasts in TEM image, so that the whole area had been further analyzed by energy dispersive spectrum (EDS). The co-dispersion and uniform mixing of multi-component system was obtained which was confirmed in Fig. 13b. The EDS exhibits that ZrB_2 and SiC nanopowders were well mixed with each other. The average particle size of co-dispersed powders was about 0.32 μm after dispersion treatment (Fig. 13c). This result was consistent with the single-phase experiment which the D_{50} of ZrB_2 and SiC were about 0.33 μm and 0.28 μm, respectively.

4. Conclusions

In this paper, the dispersion and co-dispersion of ZrB_2 and SiC nanopowders in ethanol solution were investigated and the following conclusions can be presented:

(1) The dispersion behavior of ZrB_2 and SiC nanopowders in ethanol solution was strongly dependent on the pH values, types and amounts of dispersant. PEI(10000) was found to be effective for the dispersion of both ZrB_2 and SiC nanopowders.
(2) The stability of ZrB_2 suspension increased as the content of PEI increased until reached 0.7 wt% and well-dispersed SiC slurry can be obtained by the application of more than 2.5 wt% PEI. When adding more than 0.7 wt% PEI into ZrB_2 suspension, the adsorption curve reached a plateau corresponding to the saturated adsorption.
(3) The IEP of ZrB_2 and SiC nanopowders in ethanol solution were at pH 10 and pH 9.5, and then shift to pH 13 and pH 12.3 with the addition of PEI. With a certain amount of PEI,

the ZrB_2 suspension can maintain stable until around pH 12 and the agglomeration phenomenon of SiC powders did not occur below pH 10.

(4) Based on the results of the single-phase powder dispersion, the co-dispersion and uniform mixing of ZrB_2 and SiC nanocomposite powders can be at last obtained by using 1 wt% or more PEI below pH 10 which was confirmed by TEM analysis.

Acknowledgements

This work was supported by the National Science Foundation (51072042 and 50972029) of China, the Key Laboratory Opening Funding of National Key Laboratory on Advanced Composites in Special Environment (HIT.KLOF.2009026), and the Fundamental Research Funds for the Central Universities (HIT.NSRIF.2012030).

References

[1] S.R. Levine, E.J. Opila, M.C. Halbig, J.D. Kiser, M. Singh, J.A. Salem, Evaluation of ultra high temperature ceramics for aeropropulsion use, J. Eur. Ceram. Soc. 22 (14–15) (2002) 2757–2767.

[2] M.M. Opeka, I.G. Talmy, J.A. Zaykoski, Oxidation-based materials selection for 2000 °C + hypersonic aerosurfaces: theoretical considerations and historical experience, J. Mater. Sci. 39 (19) (2004) 5887–5904.

[3] C. Morz, Annual mineral review: zirconium diboride, Am. Ceram. Soc. Bull. 73 (6) (1994) 141–142.

[4] K. Upadhya, J.M. Yang, W.P. Hoffman, Materials for ultrahigh temperature structural applications, Am. Ceram. Soc. Bull. 76 (12) (1997) 51–56.

[5] F. Monteverde, A. Bellosi, Development and characterization of metal-diboride-based composites toughened with ultra-fine SiC particulates, Solid State Sci. 7 (5) (2005) 622–630.

[6] Y.J. Yan, Z.R. Huang, S.M. Dong, D.L. Jiang, Pressureless sintering of high-density ZrB_2–SiC ceramic composites, J. Am. Ceram. Soc. 89 (11) (2006) 3589–3592.

[7] H.W. Song, S.R. Guo, Z.Q. Hu, A coherent polycrystal model for the inverse Hall–Petch relation in nanocrystalline materials, Nanostruct. Mater. 11 (2) (1999) 203–210.

[8] Q. Liu, W.B. Han, P. Hu, Microstructure and mechanical properties of ZrB_2–SiC nanocomposite ceramic, Scr. Mater. 61 (2009) 690–692.

[9] Q. Liu, W.B. Han, J.C. Han, Influence of SiCnp content on the microstructure and mechanical properties of ZrB_2–SiC nanocomposite, Scr. Mater. 63 (2010) 581–584.

[10] Z.Y. Lu, G. Wang, J.Q. Zhuang, W.S. Yang, Effects of the concentration of tetramethylammonium hydroxide peptizer on the synthesis of Fe_3O_4/SiO_2 core/shell nanoparticles, Colloids Surf. A 278 (1–3) (2006) 140–143.

[11] A.S. Nair, T. Pradeep, I. MacLaren, An investigation of the structure of stearate monolayers on Au@ZrO_2 and Ag@ZrO_2 core–shell nanoparticles, J. Mater. Chem. 14 (2004) 857–862.

[12] J. Ren, W.M. Wang, S.C. Lu, J. Shen, F.Q. Tang, Characteristics of dispersion behavior of fine particles in different liquid media, Powder Technol. 137 (1–2) (2003) 91–94.

[13] J. Lai, K.V.P.M. Shafi, A. Ulman, et al., One-step synthesis of core(Cr)/shell(g-Fe_2O_3) nanoparticles, J. Am. Chem. Soc. 127 (16) (2005) 5730–5731.

[14] Z.H. Lü, D.L. Jiang, J.X. Zhang, Q.L. Lin, Processing and properties of ZrB_2–SiC composites obtained by aqueous tape casting and hot pressing, Ceram. Int. 37 (1) (2011) 293–301.

[15] V. Medri, C. Capiani, D. Gardini, Slip casting of ZrB_2–SiC composite aqueous suspensions, Adv. Eng. Mater. 12 (3) (2010) 210–215.

[16] S.C. Zhang, G.E. Hilmas, W.G. Fahrenholtz, Pressureless densification of zirconium diboride with boron carbide additions, J. Am. Ceram. Soc. 89 (5) (2006) 1544–1550.

[17] S.K. Mishra, S.K. Das, Sintering and microstructural behavior of SHS produced zirconium diboride powder with the addition of C and TiC, Mater. Lett. 59 (27) (2005) 3467–3470.

[18] S.H. Lee, Y. Sakka, Y. Kagawa, Corrosion of ZrB_2 powder during wet processing—analysis and control, J. Am. Ceram. Soc. 91 (5) (2008) 1715–1717.

[19] T.S. Huang, G.E. Hilmas, W.G. Fahrenholtz, Dispersion of zirconium diboride in an aqueous, high-solids paste, Int. J. Appl. Ceram. Technol. 4 (5) (2007) 470–479.

[20] A. Pettersson, G. Marino, A. Pursiheimo, J.B. Rosenholm, Electrosteric stabilization of Al_2O_3, ZrO_2, and 3Y-ZrO_2 suspensions: effect of dissociation and type of polyelectrolyte, J. Colloid Interface Sci. 228 (1) (2000) 73–81.

[21] G.H. Wang, P.S. Nicholson, Heterocoagulation in ionically stabilized mixed-oxide colloidal dispersions in ethanol, J. Am. Ceram. Soc. 84 (6) (2001) 1250–1256.

[22] T. Kakui, T. Miyauchi, H. Kamiya, Analysis of the action mechanism of polymer dispersant on dense ethanol alumina suspension using colloidal probe AFM, J. Eur. Ceram. Soc. 25 (5) (2005) 655–661.

[23] S. Lee, Y. Sakka, Y. Kagawa, Dispersion behavior of ZrB_2 powder in aqueous solution, J. Am. Ceram. Soc. 90 (11) (2007) 3455–3459.

[24] J. Sun, L. Gao, Dispersing SiC powder and improving its rheological behaviour, J. Eur. Ceram. Soc. 21 (13) (2001) 2447–2451.

[25] F.Q. Tang, X.X. Huang, Y.F. Zhang, J.K. Guo, Effect of dispersants on surface chemical properties of nano-zirconia suspensions, Ceram. Int. 26 (1) (2000) 93–97.

[26] M. Yang, C.M. Neubauer, H.M. Jennings, Interparticle potential and sedimentation behavior of cement suspensions review and results from paste, Adv Cem. Based Mater. 5 (1) (1997) 1–7.

[27] S. Baklouki, C. Pagnoux, T. Chartier, J.F. Baumard, Processing of aqueous α-Al_2O_3, α-SiO_2, α-SiC suspensions with polyelectrolytes, J. Eur. Ceram. Soc. 17 (12) (1997) 1387–1392.

[28] L.M. Wang, W.C. Wei, Colloidal processing and liquid-phase sintering of SiC, J. Ceram. Soc. Jpn. 103 (5) (1995) 434–443.

[29] X. Zhu, F. Tang, T.S. Suzuki, Y. Sakka, Role of the initial degree of ionization of polyethylenimine in the dispersion of silicon carbide nanoparticles, J. Am. Ceram. Soc. 86 (1) (2003) 189–191.

[30] Z.H. Lü, D.L. Jiang, J.X. Zhang, Q.L. Lin, Aqueous tape casting of zirconium diboride, J. Am. Ceram. Soc. 92 (10) (2009) 2212–2217.

[31] G.H. Wang, P. Sarkar, P.S. Nicholson, Influence of acidity on the electrostatic stability of alumina suspensions in ethanol, J. Am. Ceram. Soc. 80 (4) (1997) 965–972.

[32] Z.P. Xie, J.T. Ma, Q. Xu, Y. Huang, Y.B. Cheng, Effects of dispersants and soluble counter-ions on aqueous dispersibility of nano-sized zirconia powder, Ceram. Int. 30 (2) (2004) 219–224.

[33] J. Wang, L. Gao, Investigation of interactions between polymer-coated nano-Y-TZP particles by AFM, J. Mater. Sci. Lett. 18 (3) (1999) 181–183.